Bioorganic & Medicinal Chemistry Letters 19 (2009) 2116–2120

Contents lists available at ScienceDirect

Bioorganic & Medicinal Chemistry Letters

journal homepage: www.elsevier.com/locate/bmcl

Relationships between the structures of flavanone derivatives and their effects in enhancing Early growth response-1 gene expression

Sunhee Lee [a], Yoonkyung Woo [a], Soon Young Shin [b], Young Han Lee [b,*], Yoongho Lim [a,*]

[a] Division of Bioscience and Biotechnology, BMIC, RCD, Konkuk University, Seoul 143-701, Republic of Korea
[b] Department of Biomedical Science and Technology, RCTC, Konkuk University, Seoul 143-701, Republic of Korea

ARTICLE INFO

Article history:
Received 2 January 2009
Revised 3 March 2009
Accepted 5 March 2009
Available online 10 March 2009

Keywords:
QSAR
Flavanone

ABSTRACT

To identify the structural requirements that are pivotal in enhancing Early growth response-1 (Egr-1) expression, the quantitative relationships between the structural properties of flavanone derivatives and their increments of Egr-1 expression were elucidated using comparative molecular field analysis and comparative molecular similarity indices analysis.

Early growth response-1 (Egr-1) is an immediate-early response gene encoding a Cys2-His2-type zinc-finger transcription factor, which is induced rapidly by diverse extracellular stimuli, including genotoxic stress, injury, cytokines, and mitogens.[1] Egr-1 controls cell growth and apoptosis in many cell types by regulating the expression of genes such as *p53*, *p21Waf1/Cip1*, transforming growth factor-β1, phosphatase and tensin homolog gene, growth arrest- and DNA damage-inducible gene, *GADD45*, and fibronectin.[2,3] Egr-1 is poorly or not expressed in certain tumor cells, and the lack of Egr-1 expression is closely associated with tumor formation.[4] In contrast, ectopic overexpression of Egr-1 in tumor cells results in the suppression of cell proliferation and tumorigenicity.[5] These findings support the notion that Egr-1 functions as a tumor suppressor. Based on these studies, compounds capable of enhancing Egr-1 expression can be applied as an indicator to screen candidates for anticancer therapy.

Many natural products, such as curcumine and platycodon D are known to regulate Egr-1.[6,7] Other natural products, such as naringenin, hesperetin, and hesperidin exhibit inhibition of human breast cancer cell proliferation, cell cycle arrest, and reduction of in vivo metastatic potential, respectively.[8–10] Therefore, we tested whether these compounds, which all belong to the flavanone subgroup, can induce Egr-1 expression. Flavanone is a member of the flavonoids, which are polyphenol compounds found in plants as secondary metabolites. Typically, people uptake about 50–150 mg/day of flavonoids from vegetables, fruits, and other food sources.[11] Based on structural diversity, flavonoids are divided into several subgroups. One of these subgroups, flavanone, has a chroman-4-one moiety and is known to have an inhibitory effect on tumors.[12] As noted, naringenin, hesperetin, and hesperidin belong to the flavanone subgroup, yet they exhibit different biological activities. Studies on the relationships between the structures of flavanone compounds such as naringenin, hesperetin, and hesperidin and their effects on Egr-1 expression may help us to design compounds that are more effective in Egr-1 expression. The goal of this study was to determine the structural requirements that are pivotal in enhancing Egr-1 expression.

To investigate the relationships between the structures of the compounds and their biological activities, the biological activities of the test compounds were first examined. Increments of Egr-1 expression were determined for 37 flavanone derivatives using transient transfection, promoter reporter assay,[13] and Western blot analyses.[14] The three-dimensional quantitative structure–activity relationships (3D-QSAR) were examined using the SYBYL 7.3 program.[15] The 37 compounds were divided into two groups: a training set of 29 compounds to create QSAR models, and a test set of eight compounds (**30**–**37** in Table 1) to validate the models. The structures of the 37 flavanone derivatives and their effects on Egr-1 expression are given in Table 1.

All flavanone derivatives were purchased from Indofine Chemical Co. Inc. (Hillsborough, NJ). Naringenin and hesperetin, but not dihydrorobinetin and pinocembrin, significantly increased the Egr-1 expression. To investigate the relationship between the structures of flavanone derivatives and their effects on Egr-1 expression, computational methods were applied.

Flavonoids consist of a C6–C3–C6 skeleton. In the case of flavanone, the C6–C3–C6 skeleton is composed of three rings named A-, C-, and B-rings, respectively. The 3D structures of the compounds

* Corresponding authors.
E-mail addresses: yhlee58@konkuk.ac.kr (Y.H. Lee), yoongho@konkuk.ac.kr (Y. Lim).

0960-894X/$ - see front matter © 2009 Elsevier Ltd. All rights reserved.
doi:10.1016/j.bmcl.2009.03.017

Table 1
Structures of the 37 flavanone derivatives and their effects on Egr-1 expression

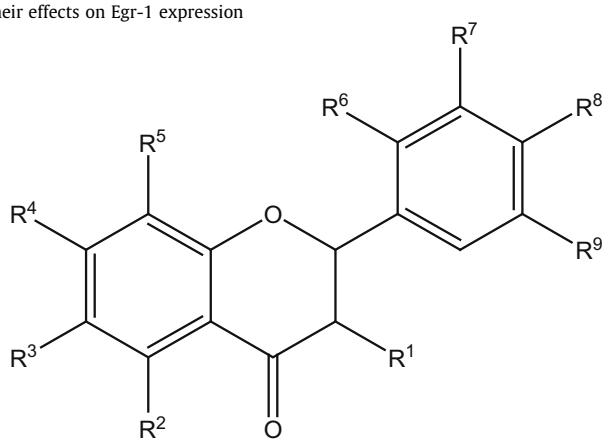

Training set	Nomenclature	R^1	R^2	R^3	R^4	R^5	R^6	R^7	R^8	R^9	Biological activity
1	5,7,4′-Trihydroxyflavanone (naringenin)	H	OH	H	OH	H	H	H	OH	H	1.2
2	5,7,3′-Trihydroxy-4′-methoxy flavanone (hesperetin)	H	OH	H	OH	H	H	OH	OMe	H	2.4
3	5,7-Dihydroxy-3′,4′,5′-trimethoxyflavanone	H	OH	H	OH	H	H	OMe	OMe	OMe	1.2
4	3,7,3′,4′,5′-Pentahydroxyflavanone (dihydrorobinetin)	OH	H	H	OH	H	H	OH	OH	OH	0.7
5	6,2′-Dihydroxyflavanone	H	H	OH	H	H	OH	H	H	H	1.2
6	5,7,3′,4′-Tetrahydroxyflavanone (eriodictyol)	H	OH	H	OH	H	H	OH	OH	H	2.1
7	3,5,7,3′,4′-Pentahydroxyflavanone	OH	OH	H	OH	H	H	OH	OH	H	1.3
8	3,7,3′4′-Tetrahydroxyflavanone	OH	H	H	OH	H	H	OH	OH	H	1.3
9	2′-Hydroxyflavanone	H	H	H	H	H	OH	H	H	H	4.2
10	3′-Hydroxyflavanone	H	H	H	H	H	H	OH	H	H	6.7
11	6-Hydroxyflavanone	H	H	OH	H	H	H	H	H	H	1.3
12	7-Hydroxyflavanone	H	H	H	OH	H	H	H	H	H	2.1
13	5-Methoxyflavanone	H	OMe	H	H	H	H	H	H	H	3.6
14	7-Methoxyflavanone	H	H	H	OMe	H	H	H	H	H	1.1
15	3′,4′-Dimethoxyflavanone	H	H	H	H	H	H	OMe	OMe	H	4.3
16	5,7-Dimethoxyflavanone	H	OMe	H	OMe	H	H	H	H	H	1.9
17	4′-Hydroxy-3′-methoxyflavanone	H	H	H	H	H	H	OMe	OH	H	5.1
18	6,2′,3′-Trimethoxyflavanone	H	H	OMe	H	H	OMe	OMe	H	H	3.9
19	6,2′,4′-Trimethoxyflavanone	H	H	OMe	H	H	OMe	H	OMe	H	1.5
20	6,3′,4′-Trimethoxyflavanone	H	H	OMe	H	H	H	OMe	OMe	H	0.7
21	4′-Methoxyflavanone	H	H	H	H	H	H	H	OMe	H	1.2
22	6,3′-Dimethoxyflavanone	H	H	OMe	H	H	H	OMe	H	H	2.5
23	5,7,4′-Trimethoxyflavanone	H	OMe	H	OMe	H	H	H	OMe	H	0.7
24	7,3′,4′,5′-Tetramethoxyflavanone	H	H	H	OMe	H	H	OMe	OMe	OMe	1
25	5,4′-Dihydroxy-7-*o*-methoxyflavanone	H	OH	H	OMe	H	H	H	OH	H	0.4
26	8-Chloroflavanone	H	H	H	H	Cl	H	H	H	H	1.7
27	8-Chloro-4′-fluoroflavanone	H	H	H	H	Cl	H	H	F	H	2.4
28	6-Chloro-4′-methylflavanone	H	H	Cl	H	H	H	H	Me	H	0.8
29	8-Chloro-4′-methylflavanone	H	H	H	H	Cl	H	H	Me	H	1.3
Test set											
30	5,7,4′-Trihydroxy-3′-methoxyflavanone (homoeriodictyol)	H	OH	H	OH	H	H	OMe	OH	H	1.2
31	5,7-Dihydroxyflavanone (pinocembrin)	H	OH	H	OH	H	H	H	H	H	0.4
32	Flavanone	H	H	H	H	H	H	H	H	H	2.3
33	4′-Hydroxyflavanone	H	H	H	H	H	H	H	OH	H	1.4
34	6-Methoxyflavanone	H	H	OMe	H	H	H	H	H	H	1.6
35	5-Hydroxy-7-methoxyflavanone	H	OH	H	OMe	H	H	H	H	H	1.6
36	7-Hydroxy-5-methoxyflavanone	H	OMe	H	OH	H	H	H	H	H	1
37	6-Chloro-3′,4′-dimethoxyflavanone	H	H	Cl	H	H	H	OMe	OMe	H	0.7

Biological activity is the level observed when treated with the compounds compared to the level of the control, in which the control level without flavanone compounds was considered as **1**.

used here were then determined. In this experiment, an ab initio method was adapted using the GAUSSIAN 98 program. Because all 37 compounds used in this experiment have chromen-4-one, the calculation was performed ab initio.[16] This structure agreed with the A- and C-rings of naringenin obtained from X-ray crystallography as a ligand for multidrug binding protein Ttgr (PDB code 2UXU).[17] All compounds were built up using chrome-4-one, and then subjected to energy minimization.

All compounds were aligned using the DATABASE Alignment module in the SYBYL program. In the alignment procedure, compound **10**, showing the best activity value, was used as a template and the atom-based root mean square (rms) fit method with DATABASE ALIGN option in SYBYL was adapted.[17] A training set was used for comparative molecular field analysis (CoMFA).[18] Since comparative molecular similarity indices analysis (CoMSIA) can calculate the steric and electrostatic fields as well as the hydrophobic, hydrogen bond (H-bond) donor, and H-bond acceptor fields, the contour maps obtained from CoMSIA were useful.[19] The partial least square (PLS) analysis was carried out to examine the correlation between the biological activities and descriptors showing the physicochemical properties of the compounds.[20]

Among the several models generated from CoMFA, the model showing the best cross-validated value ($q^2 = 0.687$) was chosen.[17] To establish a linear relationship between the biological activity

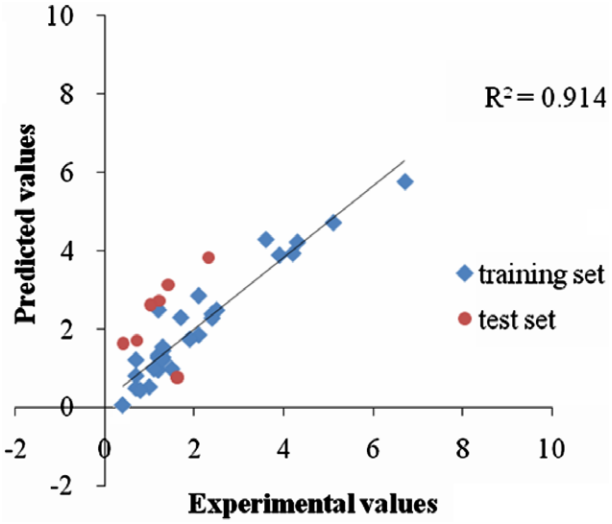

Figure 1. Correlation between experimental and predicted values from the CoMFA model.

and the resulting field matrix of the compounds, PLS analysis was carried out. The cross-validated analysis was performed using the leave-one-out (LOO) method. The final non-cross-validated (r^2) analysis was performed using the optimal number of components obtained from the LOO method. In this experiment, the r^2 value was 0.914. The best CoMFA model was obtained with a region focusing method. To check the CoMFA model, the activities of the compounds contained in the training set were predicted and compared to the experimental data (Fig. 1). The residual values between the experimental and predicted values for the training set ranged from 0.012 to 1.293.[17] Since the biological data used in this experiment were obtained from a cell-based assay, the range of error could be larger than that obtained with a molecular assay. To validate the QSAR model, a test set was selected. The residual values between the experimental and predicted values for the test set were less than 1.739.[17]

Among the several models generated from CoMSIA, the model displaying the best cross-validated value ($q^2 = 0.594$) was selected.[17] The corresponding r^2 was 0.909. The residual values between the experimental and predicted values for the training set ranged from 0.002 to 1.455.[17] The residual values between the experimental and predicted values for the test set were less than 2.148.[17]

To visualize the relationships between the structures and their activities, CoMFA contour maps were generated using SYBYL 7.3. The steric and electrostatic contributions are depicted in Figure 2. In the case of the steric field, the steric bulky favored region contributed 65% and the disfavored region 35% (Fig. 2). The bulky favored region contained the 2′- and 3′-positions of the B-ring and the 5-position of the A-ring; the bulky disfavored region included the 6-position of the A-ring. In the electrostatic field, the electronegative favored region contributed 65% and the electropositive favored region 35%. The electropositive region contained the 4′-position of the B-ring and the 5- and 6-positions of the A-ring.

To obtain information on the steric, electrostatic, and hydrophobic properties, CoMSIA contour maps were generated (Fig. 3). Even though CoMSIA can give information about the steric and electrostatic fields, as well as the hydrophobic, hydrogen bond (H-bond) donor, and H-bond acceptor fields, the result in this experiment provided from the CoMSIA calculations gave us information about the steric, electrostatic, and hydrophobic fields.

In the case of the steric field, the steric bulky favored region contributed 80% and the disfavored region 20%. The bulky favored region contained 2′- and 3′-positions of the B-ring and the 5-position of the A-ring; the bulky disfavored region was near the 4′-position of the B-ring and the 6-position of the A-ring. In the electrostatic field, the electronegative favored region contributed 78% and the electropositive favored region 22%. The electropositive region contained the 4′-position of the B-ring and the 6-position of the A-ring, while the electronegative region was near the 2′-and 3′-positions of the B-ring. The steric and electrostatic contour maps

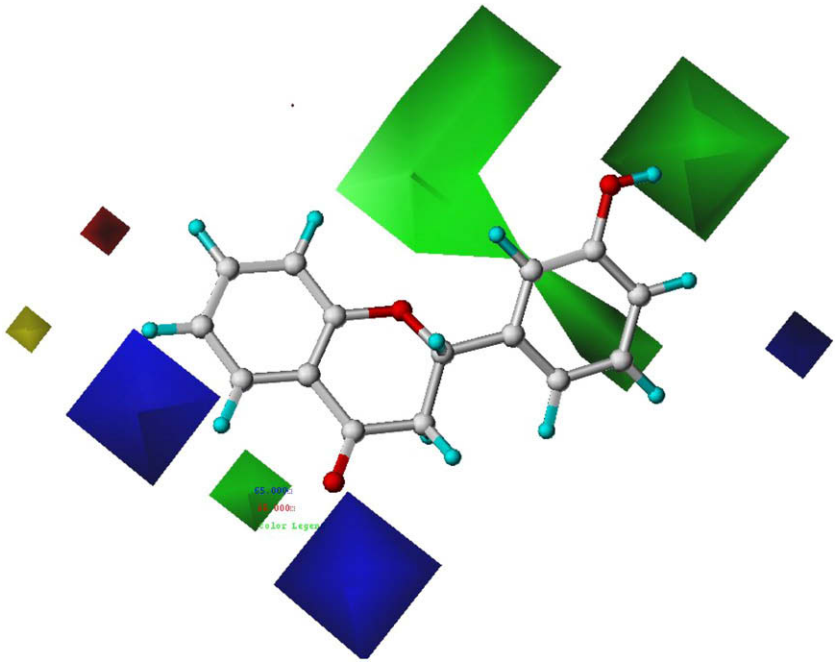

Figure 2. CoMFA contour maps. The corresponding steric and electrostatic field contributions are 85.8% and 14.2%, respectively. The steric field contours are shown in green (more bulk favored) and yellow (less bulk favored), while the electrostatic field contours are shown in red (electronegative substituent favored) and blue (electropositive substituent favored).

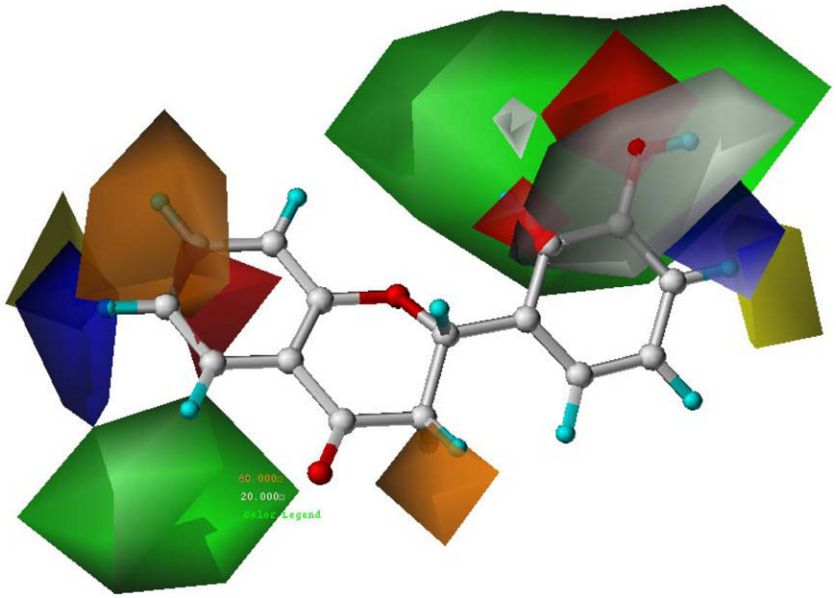

Figure 3. CoMSIA contour maps. More bulk favored (green), less bulk favored (yellow), electronegative favored (red), electropositive favored (blue), hydrophobic favored (orange), and hydrophilic favored (white) contours are shown in CoMSIA contour maps. The corresponding field contributions of steric, electrostatic, and hydrophobic are 11.1%, 55.3%, and 33.6%, respectively.

from CoMSIA analysis were generally in accordance with the CoMFA contour maps. Thus, the CoMSIA result focused on the hydrophobic field. The hydrophobic contour map indicates orange contours (hydrophobic substituent favored) and white contours (hydrophilic substituent favored). In the case of the hydrophobic field, the hydrophobic favored region contributed 80% and the hydrophilic region 20%. The hydrophobic favored region contained the 3-position of the C-ring, and the 6- and 7-positions of the A-ring; the hydrophilic region was near the 2′- and 3′-positions of the B-ring.

The ranges of residuals obtained from the experimental and predicted values were not small. Hence, to determine whether the results obtained were reliable, human cervix carcinoma HeLa cells were either untreated or treated with different concentrations of compounds (10, 20, or 40 μM) for 1 h and the level of Egr-1 expression was examined by Western blot analysis. As shown in Figure 4, the level of Egr-1 increased substantially upon treatment with **9**, **10**, or **13**, of which the predicted values were 3.930, 5.756, or 4.283, respectively. These data suggest that the predicted values deduced from CoMFA and CoMSIA models can be used to predict the unknown property in Egr-1 gene expression.

Flavonoids such as (−)-epicatechin gallate, quercetin, and genistein are involved in regulating Egr-1.[21–23] Of flavanones, pinocembrin and naringenin induce apoptosis, but the effects of flavanone on Egr-1 expression are not fully understood.[24,25] Here, the authors report the effects of 37 flavanone derivatives on the level of Egr-1 expression. In particular, the relationships between the structural properties of flavanones and their effects on Egr-1 obtained in this experiment may help to better design a novel compound that can effectively induce Egr-1 expression.

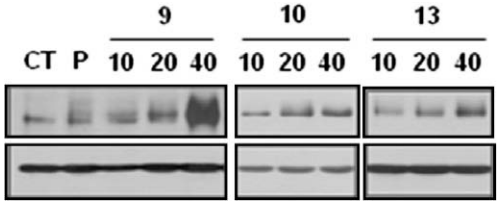

Figure 4. Human cervix carcinoma HeLa cells either untreated or treated with different concentrations of compounds (10, 20, or 40 μM) for 1 h and the level of Egr-1 expression was examined by Western blot analysis.

Acknowledgments

This work was supported by Grant KRF-2006-005-J03402 (KRF), Grant M10751050003-07N5105-00310 (KOSEF), Grant Biogreen 21 (RDA), and Agenda 11-30-68 (NIAS). We appreciate Dr. K.S. Lee (NIH) for his suggestion.

Supplementary data

Supplementary data associated with this article can be found, in the online version, at doi:10.1016/j.bmcl.2009.03.017.

References and notes

1. Ariel, Q.; Karl, U. D.; Nikolai, G. R. *Life Sci.* **2003**, *72*, 2975.
2. Veronique, B.; Eileen, D. A.; Antonella, C.; Giuseppe, R.; Dan, M. *Cancer Gene Ther.* **2005**, *13*, 115.
3. Sandra, F.; Salatiel, M.; Lebreton-De, C.; Michèle, O.; Louis, D.; Bernard, C. *EMBO J.* **2005**, *24*, 128.
4. Huang, R. P.; Fan, Y.; de Belle, I.; Niemeyer, C.; Gottardis, M. M.; Mercola, D.; Adamson, E. D. *Int. J. Cancer* **1997**, *72*, 102.
5. Scharnhorst, V.; Menke, A. L.; Attema, J.; Haneveld, J. K.; Riteco, N.; van Steenbrugge, G. J.; van der Eb, A. J.; Jochemsen, A. G. *Oncogene* **2000**, *19*, 791.
6. Pendurthi, U. R.; Rao, L. V. *Thromb. Res.* **2000**, *97*, 179.
7. Choi, W. Y.; Kim, G. Y.; Lee, W. H.; Choi, Y. H. *Chemotherapy* **2008**, *54*, 279.
8. So, F. V.; Guthrie, N.; Chambers, A. F.; Moussa, M.; Carroll, K. K. *Nutr. Cancer* **1996**, *26*, 167.
9. Choi, E. J. *Nutr. Cancer* **2007**, *59*, 115.
10. Lentini, A.; Forni, C.; Provenzano, B.; Beninati, S. *Amino Acids* **2007**, *32*, 95.
11. Salucci, M.; Stivala, L. A.; Maiani, G.; Bugianesi, R.; Vannini, V. *Br. J. Cancer* **2002**, *86*, 1645.
12. Ko, C. H.; Shen, S. C.; Lin, H. Y.; Hou, W. C.; Lee, W. R.; Yang, L. L.; Chen, Y. C. *J. Cell. Physiol.* **2002**, *193*, 93.
13. Human embryonic kidney (HEK) 293 cell was obtained from the American Type Culture Collection (Manassas, VA) and maintained in Dulbecco's modified Eagle's medium (DMEM) supplemented with 10% fetal bovine serum (FBS; Hyclone, Logan, UT). For the promoter reporter assay, HEK293 cell was seeded onto 12-well plates and transfected with 0.5 μg of Pegr1-Luc, an Egr-1 promoter containing construct,[26] using LipofectAMINE 2000 reagent

(Invitrogen Life Technologies, San Diego, CA). To monitor the transfection efficiency, a pRL-null plasmid (50 ng) encoding *Renilla* luciferase was included in all transfections. At 24 h post-transfection, cells were treated with flavanone derivatives (20 μg/mL). After 6–12 h, the levels of firefly and *Renilla* luciferase activity were measured sequentially from a single sample using the Dual-Glo Luciferase Assay System (Promega, Madison, WI) with a luminometer (Centro LB960; Berthold Technologies GmbH, Bad Wildbad, Germany). The level of a control without flavanone compounds was considered as **1** and the levels treated with the compounds were compared to the control.

14. To verify the Egr-1 expression, Western blot analysis was performed. HEK293 cells were serum-starved with 0.5% serum for 24 h and then treated with increasing concentrations of flavanone derivatives (0, 10, 20, or 40 μg/mL) for 1 h. Cells were lysed in buffer (20 mM HEPES [pH 7.2], 1% Triton X-100, 10% glycerol, 150 mM NaCl, 10 μg/mL leupeptin, 1 mM PMSF). The protein extracts (20 μg each) were separated by 10% SDS–polyacrylamide gel electrophoresis and transferred to nitrocellulose filters. The blots were incubated with the anti-Egr-1 or anti-GAPDH antibody, and then developed using an enhanced chemiluminescence detection system (Amersham Pharmacia Biotech, Piscataway, NJ).[26]
15. Kim, H.; Lee, E.; Kim, J.; Jung, B.; Chong, Y.; Ahn, J. H.; Lim, Y. *Bioorg. Med. Chem. Lett.* **2007**, *18*, 661.
16. The Becke's three-parameter hybrid method in GAUSSIAN 98 (Gaussian Inc., Wallingford, CT) with the 6-31G basis set of the density functional theory was used for geometry optimization of the compounds.[27] The structures obtained by GAUSSIAN 98 were subjected to energy minimization carried out on an Intel Core 2 Quad Q6600 (2.4 GHz) Linux PC with SYBYL 7.3 (Tripos, St. Louis, MO).[28] The minimization process was ceased at the convergence criteria of the total energy (0.05 kcal/mol A).[17]
17. Data not shown in the text can be found in Supplementary data.
18. The aligned molecules were placed in a 3D cubic lattice with a grid spacing of 2.0 Å in the *x*, *y*, and *z* directions. The steric (Lennard–Jones 6-12 potential) and electrostatic (Coulombic potential) field energies were calculated at each grid point using a Tripos force field. The energies were truncated to +30 kcal/mol. Similarity descriptors were derived according to Klebe et al. with the same grid as that used in CoMFA field calculations.[29]
19. A probe atom sp^3 carbon with charge +1, hydrophobicity +1, and H-bond donor and H-bond acceptor property of +1 was placed at every grid point to measure the five CoMSIA fields. A default value of 0.3 was used as an attenuation factor.
20. The cross-validation analysis was performed using the 'leave-one-out' (LOO) method. The optimum number of components obtained from the LOO method was applied to derive the final non-cross-validated correlation r^2. The best CoMFA model was improved by a region focusing method.
21. Choa, K. N.; Mugdha, S.; Leea, S. H.; Yoonb, J. H.; Baek, S. J. *Eur. J. Cancer* **2007**, *43*, 2404.
22. Lim, J. H.; Park, J. W.; Min, D. S.; Chang, J. S.; Lee, Y. H.; Park, Y. B.; Choi, K. S.; Kwon, T. K. *Apoptosis* **2007**, *12*, 411.
23. Singletary, K.; Ellington, A. *Anticancer Res.* **2006**, *26*, 1039.
24. Gao, M.; Zhang, W. C.; Liu, Q. S.; Hu, J. J.; Liu, G. T.; Du, G. H. *Eur. J. Pharmacol.* **2008**, *591*, 73.
25. Park, J. H.; Jin, C. Y.; Lee, B. K.; Kim, G. Y.; Choi, Y. H.; Jeong, Y. K. *Food Chem. Toxicol.* **2008**, *46*, 3684.
26. Shin, S. Y.; Bahk, Y. Y.; Ko, J.; Chung, I. Y.; Lee, Y. S.; Julian, D.; Hermann, E.; Prem, M. S.; Jerrold, M. O.; Kim, Y. H.; Lee, B.; Lee, Y. H. *EMBO J.* **2006**, *25*, 1093.
27. Schaftenaar, G.; Noordik, J. H. *J. Comput. Aided Mol. Des.* **2000**, *14*, 123.
28. Hong, S. W.; Moon, B. H.; Yong, Y. J.; Shin, S. Y.; Lee, Y. H.; Lim, Y. *J. Microbiol. Biotechnol.* **2008**, *18*, 682.
29. Klebe, G.; Abraham, U.; Mietzner, T. *J. Med. Chem.* **1994**, *37*, 4130.